Clinical Note

Juxtapapillary Diverticulum: Findings on MRI

N. Cem Balci, MD,[1]* Tara Noone, MD,[2] Elif Akün, MD,[3] Ahmet Akinci, MD,[3] and Hans-Ulrich Klör, MD[3]

The purpose of our study was to describe the imaging findings of juxtapapillary diverticulum on magnetic resonance imaging (MRI). The MRI and magnetic resonance cholangiopancreatography (MRCP) examinations of 14 patients with juxtapapillary diverticula that were diagnosed on endoscopic retrograde cholangiopancreatography (ERCP) ($N = 8$) or endoscopy ($N = 6$) were retrospectively evaluated. T1-weighted spoiled gradient-echo, T2-weighted half Fourier single shot fast spin-echo (HASTE), and T2-weighted True FISP (fast imaging with steady state precession) images and thin-slice MRCP images were obtained on all patients. In five patients, diluted gadolinium DPTA (1/100) was used as an oral contrast. T2-weighted True FISP and HASTE images demonstrated air-fluid levels within all diverticula. Hyperintense oral contrast on T1-weighted spoiled gradient-echo images aided detection of the smaller diverticula. MRCP images obtained in the coronal plane best demonstrated the relationship of the diverticula to the papilla. MRI with the use of HASTE, True FISP, and oral contrast-enhanced T1-weighted sequences was able to depict juxtapapillary diverticula in our series.

Key Words: papilla; diverticulum; MRI; MRCP; ERCP; duodenum
J. Magn. Reson. Imaging 2003;17:487–492.

A JUXTAPAPILLARY DIVERTICULUM is defined as a duodenal diverticulum within close proximity to the duodenal papilla. Some authors hypothesize that a motility disorder of the sphincter of Oddi is related to juxtapapillary diverticulum formation (1–6). They are commonly associated with concomitant biliary or pancreatic disease, including choledocholithiasis, common bile duct dilatation, cholelithiasis, and pancreatitis. The majority of juxtapapillary diverticula are discovered incidentally on barium studies or on endoscopic examinations.

Patients with juxtapapillary diverticula may undergo magnetic resonance imaging (MRI) of the upper abdomen and magnetic resonance cholangiopancreatography (MRCP) to explore their related pancreaticobiliary disease symptoms. The majority of these patients have imaging findings consistent with choledocholithiasis, cholelithiasis, and/or chronic pancreatitis, which may result from the presence of the juxtapapillary diverticulum (3,5,8,9). Juxtapapillary diverticula can alter cannulation of the papilla at ERCP; therefore, prior detection with MRI and MRCP can aid management planning (7–9). Patients who do not undergo ERCP or endoscopic examination may benefit from the ability of MRI and MRCP to detect these lesions, enabling determination of the etiology of clinical symptomatology and guidance for appropriate clinical management (5,6).

The purpose of our retrospective study was to describe the imaging findings of the juxtapapillary diverticulum on MRI and MRCP. To our knowledge, these MRI findings have not been described previously.

MATERIALS AND METHODS

From January 2001 to May 2002, a total of 30 consecutive patients (14 male, 16 female; age range 63–78 years, mean 68.3 years) were identified and underwent MRI of the upper abdomen and MRCP, in conjunction with ERCP or endoscopic examination of the duodenum. All of these patients were referred for MRI to rule out biliary and pancreatic disease. Fourteen patients were diagnosed with juxtapapillary diverticula by ERCP ($N = 8$) or endoscopy ($N = 6$), and their MRI examinations were retrospectively evaluated.

MRI was performed for the following reasons: elevation of biliary and/or pancreatic enzymes ($N = 8$), elevated liver enzymes ($N = 7$), clinical suspicion of cholecystitis ($N = 2$), clinical suspicion of malignancy ($N = 3$), and failed cannulation of the papilla at ERCP ($N = 2$). A total of eight patients underwent ERCP examination after the MRI examination. In four patients, ERCP was performed to further evaluate clinically suspected sphincter of Oddi dysfunction (SOD) or stenosis as the cause of pancreatitis, and in four patients, ERCP was performed to remove sludge from the common bile duct (CBD). Two patients underwent ERCP as the initial examination, but were then examined by MRCP because

[1]Department of Radiology, Florence Nightingale Hospital, Istanbul, Turkey.
[2]Department of Radiology, Medical University of South Carolina, Charleston, South Carolina.
[3]Department of Internal Medicine, Kadir Has University, Istanbul, Turkey.
*Address reprint request to: N.C.B., Boğazici Sitesi, A Blok, No: 13, Daire: 20, 80860, Istinye, Istanbul, Turkey.
E-mail: nc.balci@mailexcite.com
Received August 27, 2002; Accepted December 16, 2002.
DOI 10.1002/jmri.10281
Published online in Wiley InterScience (www.interscience.wiley.com).

cannulation of the papilla was not successful at ERCP. Six patients underwent endoscopy to evaluate duodenal disease. ERCP in our institution was performed in standard fashion with selective cannulation and injection of the common bile and pancreatic ducts with contrast material.

MRI was performed on a 1.5-Tesla MRI system (Magnetom Sonata; Siemens Medical Systems, Erlangen, Germany) equipped with high performance gradients (40 mT/m maximum gradient strength and 200 μsec rise time). MRI of the upper abdomen was performed with the use of a phased-array body coil. Patients had a fasting period of six hours before the examination, and one half hour before the MRI examination, five patients received an oral solution of 5 mL of Gd-DTPA added to 500 mL of tap water. The following imaging sequences were obtained in all patients: breath-hold, T1-weighted spoiled gradient echo, in phase and out of phase (repetition time [TR] = 150–170 msec, echo time [TE] = 2–4 msec, flip angle [FA] = 70°); T1-weighted fat suppressed, breath-hold, in-phase gradient-echo images (TR = 180–190 msec, TE = 4.6 msec, FA = 70°); T2-weighted half Fourier single shot fast spin echo (HASTE) with and without fat suppression (TR = ∞, TE = 90 msec) in axial and coronal planes; and T2-weighted True-FISP (fast imaging with steady state precession; TR = 3.6 msec, TE = 1.8 msec, FA = 70°) in axial and coronal planes. MRCP was performed using a thin slice HASTE (TR = ∞, TE = 90 msec) in multiple paracoronal planes with 4-mm section thickness, acquiring 14–16 sections total. Post-gadolinium images were obtained using a T1-weighted spoiled gradient-echo sequence with the same parameters as the precontrast scan. Gadolinium chelates (Magnevist, Schering, Berlin, Germany) were administered at a dose of 0.1 mmol/kg and serial contrast-enhanced images were obtained. All imaging sequences, except for the MRCP, were acquired using 14–16 sections and a section thickness of 6–8 mm. The matrix for all scans was 128–145 × 256 (phase encoding x frequency encoding).

MRI and MRCP images were reviewed retrospectively by two radiologists and by two gastroenterologists. A total of 14 juxtapapillary diverticula were visualized and retrospectively evaluated on MRI. On the cross sectional images, the location, size, and content of the diverticulum, as well as the morphology and signal intensity of the pancreatic parenchyma and biliary tract, were evaluated. For signal intensity assessment, paraspinal muscles and liver parenchyma were used as references on fat saturated images.

RESULTS

All juxtapapillary diverticula were located in the medial wall of the second portion of the duodenum. The diameters of the diverticula ranged from 1–4 cm (mean, 1.7 cm). T2-weighted images demonstrated air-fluid levels, identified by the presence of hyperintense fluid layering dependently relative to signal void air in all patients. In patients receiving oral gadolinium, diverticula were not visualized on HASTE and T2-weighted fast spin-echo images secondary to the T2 shortening effect of the oral contrast. On T2-weighted True FISP images, air-fluid levels were observed, without the signal loss of the fluid contents in patients administered oral contrast (Fig. 1). T2-weighted HASTE images and True FISP images best demonstrated the wall of the diverticulum and its relationship to the papilla (Figs. 1 and 2). The relationship of the papilla to the wall of the diverticulum was evaluated on the T2-weighted HASTE and true FISP images in the coronal and axial planes. Coronal MRCP images demonstrated the relationship between the diverticulum and the papilla (Fig. 2). In twelve patients, the communication between the duodenal wall and the diverticulum was clearly shown (Fig. 2). On T1-weighted images, air-fluid levels were visualized as hypointense fluid layering dependently relative to the signal void air. In patients with oral contrast in the duodenum, hyperintense fluid within the diverticula observed on T1-weighted images was helpful to identify two small diverticula (Fig. 1).

In three patients, an atrophic pancreatic gland was observed. In six patients, diminished signal of the pancreatic gland was observed on T1-weighted fat suppressed images as compared to the liver parenchyma. In two patients, the CBD was dilated with mild intrahepatic biliary dilatation, but no stone formation in the CBD. In three patients, multiple gallstones were detected (Fig. 1). In three patients, no associated pathology was present on MRI.

Delayed outflow of contrast was observed on ERCP in three patients on late fluoroscopic images, consistent with SOD (Fig. 2). Three patients underwent diverticulectomy. The remainder of the patients did not undergo surgical treatment.

DISCUSSION

Duodenal diverticula are outpouchings of the mucosa and muscularis mucosa through the intestinal wall. Juxtapapillary diverticula arise within a radius of 2–3 cm from the papilla of Vater (2,5). The prevalence of juxtapapillary diverticula increases with age and is reported to be as high as 27% (5). In our small study population, the prevalence was higher because we selected patients either with a known indication for ERCP or in whom pancreatic pathology was likely.

Juxtapapillary diverticula are usually depicted either at ERCP or incidentally on barium studies of the duodenum. The computed tomography (CT) findings of juxtapapillary diverticula have been described as part of larger series and case reports. The MRI findings of this entity have not been described previously. Our findings on MRI correlate well with previously described CT findings, which included detection of an air-fluid level (10,11). On MRI, both HASTE and True-FISP techniques demonstrated air-fluid levels. Previous studies have demonstrated the usefulness of these techniques for the assessment of bowel pathology. HASTE is a motion-insensitive technique and provides clear definition of the bowel wall (12–14). Imaging findings of duodenal diverticula were reviewed within a series reporting the MRI findings of a range of duodenal pathology; this study reported imaging findings similar to those of the juxtapapillary duodenal diverticula observed in this study (13). In our study, juxtapapillary diverticula were

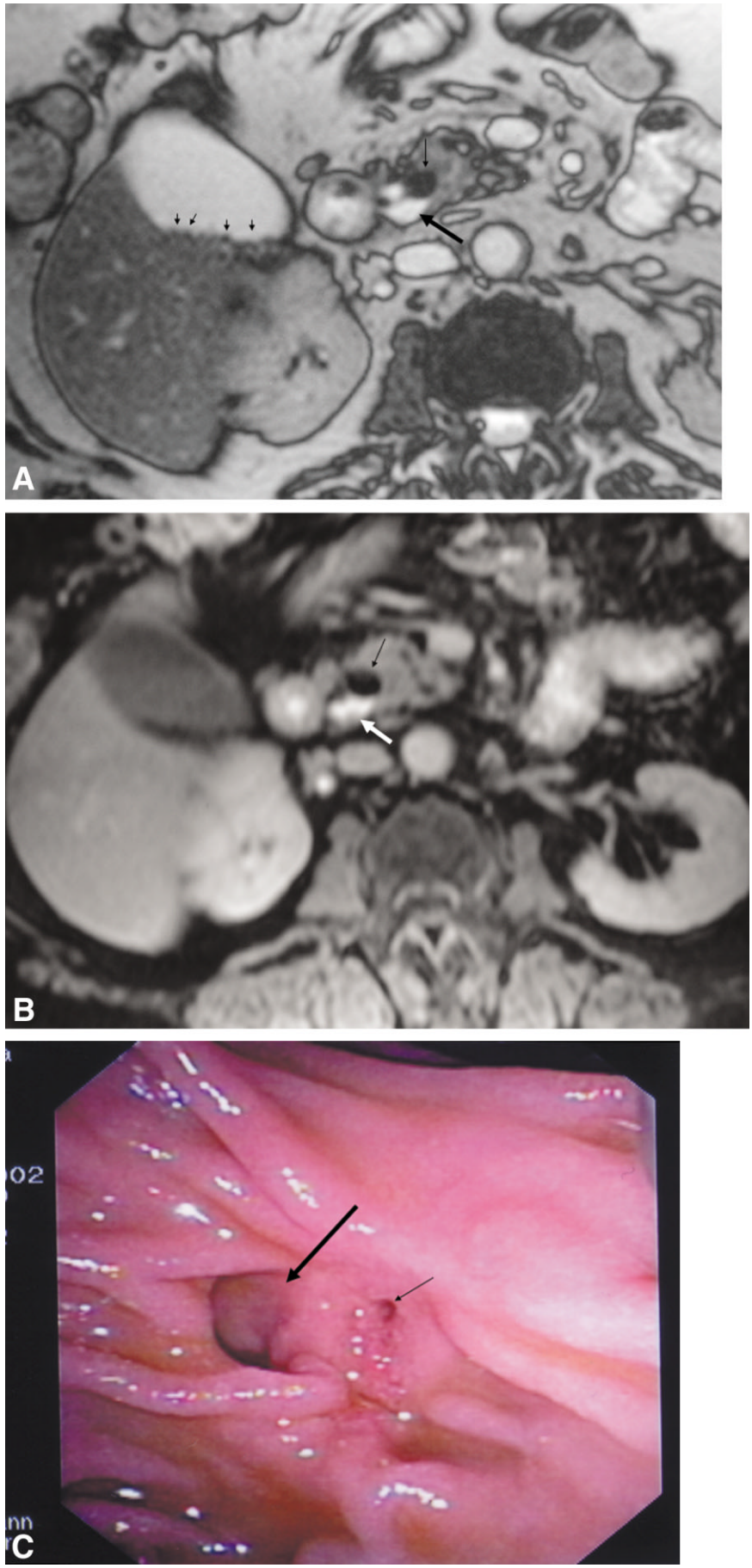

Figure 1. Small juxtapapillary diverticulum in a 67-year-old patient with multiple gallstones. T2-weighted True FISP image in the axial plane (TR = 3.6 msec, TE = 1.8 msec, FA = 70°) (**a**) reveals hyperintense fluid (long arrow) and a signal void air level (short arrow) within the diverticulum. Multiple small gallstones are observed in the gallbladder (small arrows). T1-weighted post-contrast fat suppressed spoiled gradient-echo image (TR = 165 msec, TE = 2.3 msec, FA = 70°) (**b**) in the axial plane reveals hyperintense fluid due to the oral contrast (white arrow), with a signal void air level above (black arrow). The corresponding endoscopic image during ERCP (**c**) demonstrates the diverticulum (long arrow) and its relationship to the papilla (short arrow).

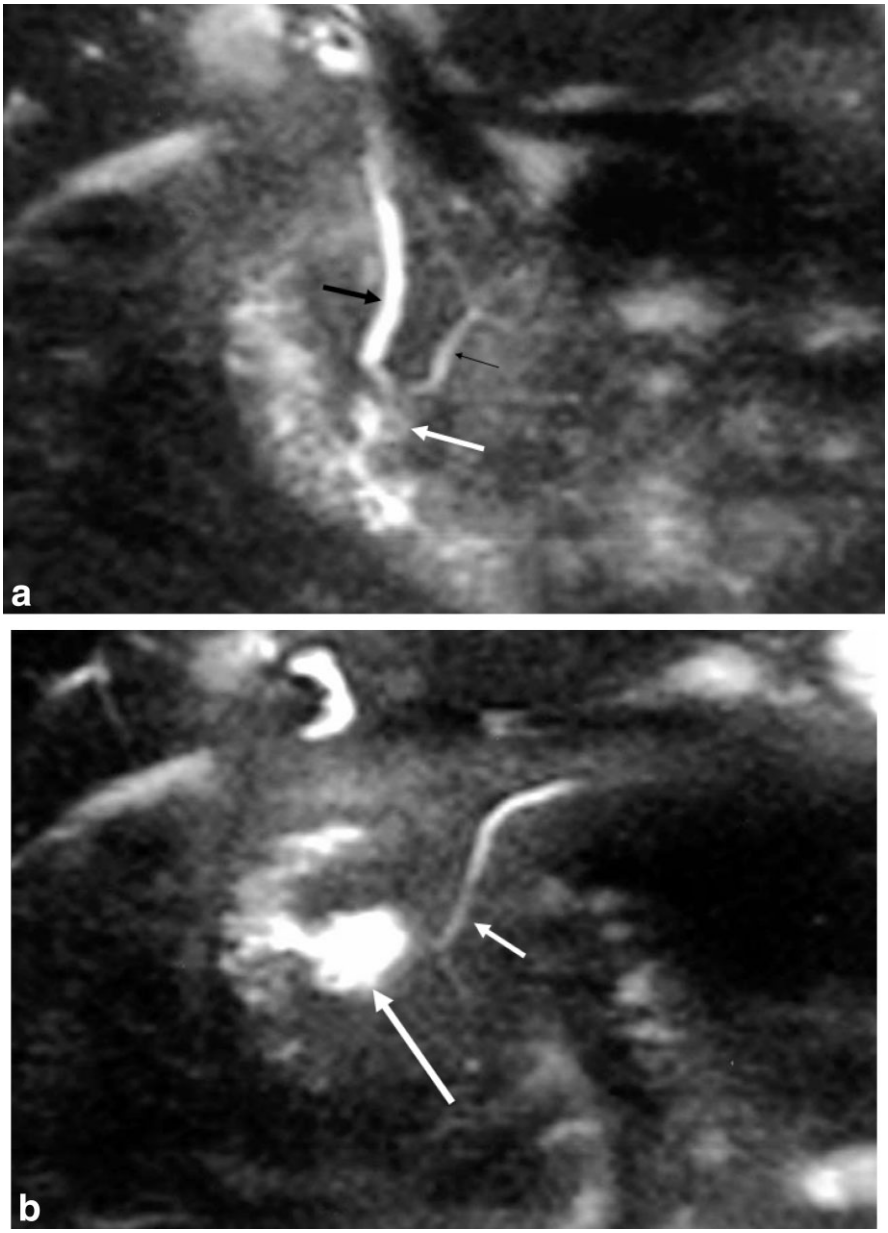

Figure 2. Juxtapapillary diverticulum in a 70-year-old patient. MRCP with the use of HASTE sequence (TR = ∞, TE = 90 msec) reveals the distal common bile duct (thick black arrow) and pancreatic duct (thin black arrow) entering into the diverticulum (white arrow) (**a**). In the next section posteriorly, (**b**) the diverticulum (long arrow) and the pancreatic duct (short arrow) are demonstrated. On the corresponding ERCP images (**c,d**), catheterization of the papilla within the diverticulum is demonstrated (c). On the late (10-minute) phase ERCP image (d), there is contrast in the CBD (thick arrow) and in the pancreatic duct (thin arrow), indicating impaired biliary outflow secondary to SOD. The juxtapapillary diverticulum is marked with a white arrow.

demonstrated on both axial and coronal sections with the HASTE technique. With the use of the strong gradient system of our scanner, a True FISP sequence with a short TR and short TE was performed, decreasing susceptibility to bowel and respiratory motion artifacts. True FISP is a fast imaging technique with steady-state precession, which provides high signal of fluid-containing structures (15). In our study, this technique enabled better delineation of the diverticular wall. It has been shown that the use of either of these techniques may be useful in the demonstration of bowel pathology (16,17).

Although the majority of juxtapapillary diverticula are asymptomatic and discovered incidentally, there are reported associations with pancreaticobiliary diseases. The most commonly associated biliary pathology is gallstone formation. This may be explained either by biliary stasis, resulting from compression of the distal CBD by the diverticulum, or by an incompetent sphincter of Oddi which causes reflux of duodenal contents. Accumulation of beta-glucuronidase producing organisms leads to formation of pigment bile stones in the CBD in patients with juxtapapillary diverticula (1,2,4). In our study, the cases associated with dilatation of the CBD revealed sludge, rather than stone formation, in the distal CBD. Three patients had multiple calculi in the gallbladder. Another disorder associated with the juxtapapillary diverticulum is pancreatitis in a chronic or acute relapsing form. This is attributed to the stasis of pancreatic secretions (1,2). Six of our patients had laboratory and imaging findings consistent with chronic pancreatitis. MRI demonstrated parenchymal signal decreases consistent with the presence of pancreatitis. Diminished signal of the pancreatic gland on T1-weighted fat saturated images associated with chronic pancreatitis has been described previously (18,19). Pancreatic cystic neoplasms and pseudocysts can be considered in the differential diagnosis with the

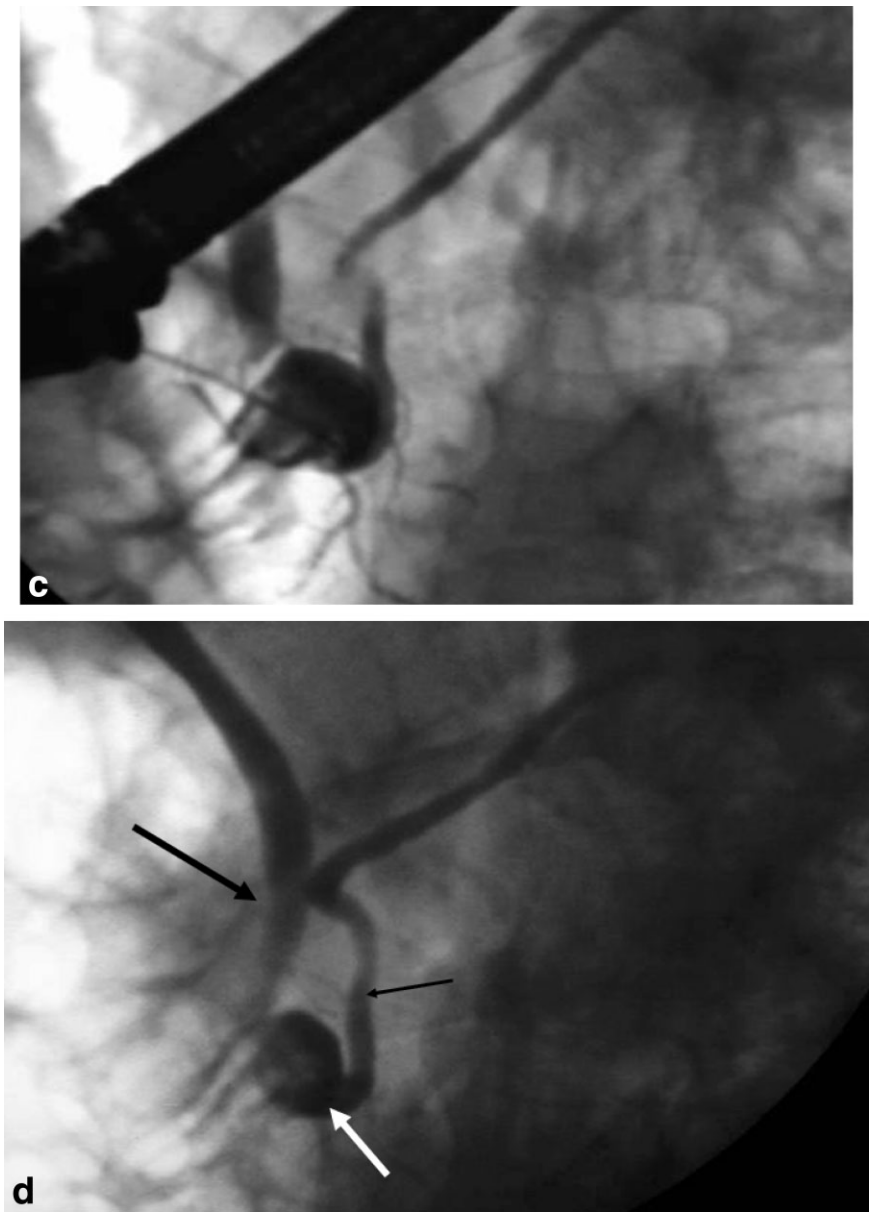

Figure 2 (Continued)

juxtapapillary diverticulum if the former are located in close proximity to the papilla (20). The air-fluid level in the diverticular sac and the demonstration of the communication between the duodenum and diverticulum are MRI features that can distinguish the diverticula from pancreatic pseudocysts and cystic neoplasms. Treatment of juxtapapillary diverticula is surgical. Either trans-abdominal or laparoscopic diverticulectomy may be performed (21). Endoscopic sphincterotomy has been used as an alternative approach for the relief of CBD stasis (6). In three of our cases, diverticulectomy was performed. As the result of short-term follow-up, resultant relief of symptoms and long-term effects of this procedure need to be investigated in larger series.

In conclusion, we described the MRI findings of juxtapapillary diverticula. T2-weighted True FISP and HASTE images best demonstrated the diverticula. Dilute oral contrast aided detection of the smaller diverticula. The associated imaging findings of pancreatitis, cholelithiasis, and dilatation of the CBD also were evaluated effectively by MRI.

REFERENCES

1. Hagege H, Berson A, Pelletier G, et al. Association of juxtapapillary diverticula with choledocholithiasis but not with cholecystolithiasis. Endoscopy 1992;24:248–251.
2. Egawa N, Kanisawa T, Tu Y, Sasaki N, Tsuruta K, Okamoto A. The role of juxtapapillary duodenal diverticulum in the formation of gallbladder stones. Hepatogastroenterology 1998;45:917–920.
3. Uomo G, Manes G, Ragozzino A, Cavellera A, Rabitti PG. Periampullary extraluminal duodenal diverticula and acute pancreatitis: an underestimated etiological association. Am J Gastroenterol 1996; 91:1186–1188.
4. Ponce J, Garrigues V, Sala T, Pertejo V, Val A, Hoyos M. Motor pattern of the sphincter of Oddi in patients with juxtapapillary diverticula. J Clin Gastroenterol 1990;12:162–165.

5. Lobo DN, Balfour TW, Iftikhar SY, Rowlands BJ. Periampullary diverticula and pancreaticobiliary disease. Br J Surg 1999;86:588–597.
6. Eapen T, Reddy KR. Cholangitis and pancreatitis due to a juxtapapillary duodenal diverticulum—endoscopic sphincterotomy is the other alternative in selected cases. Am J Gastroenterol 1982; 77:303–304.
7. Leivonen MK, Halttunen JAA, Kivilaakso EO. Duodenal diverticulum at endoscopic retrograde cholangiopancreatography: analysis of 123 patients. Hepatogastroenterology 1996;43:961–966.
8. Fujita N, Noda Y, Kobayashi G, Kimura K, Yogo A. ERCP for intradiverticular papilla: two-devices-in-one-channel method. Gastrointest Endosc 1998;48:517–520.
9. Toth E, Lindstrom E, Fork F-T. An alternative approach to the inaccessible intradiverticular papilla. Endoscopy 1999;31:554–556.
10. Stone EE, Brant WE, Smith GB. Computed tomography of duodenal diverticula. J Comput Assist Tomogr 1989;13:61–63.
11. De Rai P, Castoldi L, Tiberio G. Intraluminal duodenal diverticulum causing acute pancreatitis: CT scan and review of the literature. Dig Surg 2000;17:288–292.
12. Semelka RC, Kelekis NL, Thomasson D, Brown MA, Laub GA. HASTE MR Imaging: description of technique and preliminary results in the abdomen. J Magn Reson Imaging 1996;6:698–699.
13. Marcos HB, Semelka RC, Noone TC, Woosley JT, Lee JK. MRI of normal and abnormal duodenum using half-Fourier single-shot RARE and gadolinium-enhanced spoiled gradient echo sequences. Magn Reson Imaging 1999;17:869–880.
14. Lee JK, Marcos HB, Semelka RC. MR imaging of the small bowel using the HASTE sequence. AJR Am J Roentgenol 1998;170:1457–1463.
15. Ross JS. Newer sequences for spinal MR imaging: smorgasbord or succotash for acronyms? AJNR Am J Neuroradiolgy 1999;20:361–373.
16. Gourtsoyiannis N, Papanikolaou N, Grammatikakis J, Maris T, Prassopoulos P. MR imaging of the small bowel with a true-FISP sequence after enteroclysis with water solution. Invest Radiol 2000; 35:707–711.
17. Gourtsoyiannis N, Papanikolaou N, Grammatikakis J, Maris T, Prassopoulos P. MR enteroclysis protocol optimization: comparison between 3D FLASH with fat saturation after intravenous gadolinium injection and true FISP sequences. Eur Radiol 2001;11:908–913.
18. Semelka RC, Kroeker MA, Shoenut JP, Kroeker R, Yaffe CS, Micflikier AB. Pancreatic disease: prospective comparison of CT, ERCP, and 1.5 Tesla MR imaging with dynamic gadolinium enhancement and fat suppression. Radiology 1991;181:785–791.
19. Semelka RC, Shoenut JP, Kroeker MA, Micflikier AB. Chronic pancreatitis: MR imaging features before and after administration of gadopentetate dimeglumine. J Magn Reson Imaging 1993;3:79–82.
20. Balci NC, Semelka RC. Radiologic features of cystic, endocrine and pancreatic neoplasms. Eur J Radiol 2001;38:113–119.
21. Togaya N, Shimoda M, Hamada K, Ishikawa K, Kogure H. Laparoscopic duodenal diverticulectomy. Surg Endosc 2000;14:592–593.